# The structural and magnetic properties of $Y_{n+1}Co_{3n+5}B_{2n}$ compounds investigated by neutron diffraction

**Cyril Chacon and Olivier Isnard**

Laboratoire de Cristallographie, CNRS, associé à l'Université Joseph Fourier et à l'Institut National Polytechnique de Grenoble, BP 166, F-38042 Grenoble Cedex 9, France

**Abstract**

The crystal and magnetic structures of $Y_{n+1}Co_{3n+5}B_{2n}$ ($n = 2$, 3 and $\infty$) have been studied by high-resolution powder neutron diffraction. The results are compared to earlier measurements on $YCo_5$ and $YCo_4B$. A change in the regular stacking of the boron-containing plane along the $c$ axis has been observed in the $Y_2Co_7B_3$ sample. Very short Co–B distances are observed, indicating that strong bonds are formed between cobalt and boron. The $YCo_3B_2$ compound is paramagnetic down to 2 K. The magnetic structures of $Y_3Co_{11}B_4$ and $Y_2Co_7B_3$ confirm the large variety of cobalt magnetic moments obtained in these compounds. The magnetic behaviour of the Co(2c) atoms is not significantly affected by the substitution of boron for cobalt. Cobalt atoms with significantly reduced magnetic moments are found on the 3g and $6i_2$ sites in both $Y_3Co_{11}B_4$ and $Y_2Co_7B_3$. A relationship between the magnitude of the Co magnetic moment and the presence of boron in the neighbourhood of the cobalt atoms is proposed. The hybridization of the cobalt 3d electronic state with the boron 2p state is found to play a major role in the determination of the magnitude of the Co magnetic moment in the $Y_{n+1}Co_{3n+5}B_{2n}$ compounds.

## 1. Introduction

Rare earth (R)–transition metal (M) intermetallic compounds, such as $SmCo_5$ or $Nd_2Fe_{14}B$, form an important class of materials that find applications in permanent magnets [1]. The 3d sublattice is responsible for both the high saturation magnetization and the Curie temperature, whereas the 4f sublattice provides a rather high magnetocrystalline anisotropy.

Since their discovery [2], $R_{n+1}Co_{3n+5}B_{2n}$ ($n = 1$, 2, 3 and $\infty$) compounds have attracted interest because they form a unique series of crystal structures for different $n$ values. The $R_{n+1}Co_{3n+5}B_{2n}$ compounds are derived from $RCo_5$ by an ordered substitution of boron for cobalt. The unit cells are formed by an alternative stacking of one layer of $RCo_5$ and $n$ layers of $RCo_3B_2$ unit cells (figure 1). They all have hexagonal symmetry and crystallize in the $P6/mmm$ space group. Whereas only one rare earth site is found in the $RCo_3B_2$ structure, the $RCo_4B$ and $R_3Co_{11}B_4$ compounds are composed of two distinct R sites, the 1a and 1b
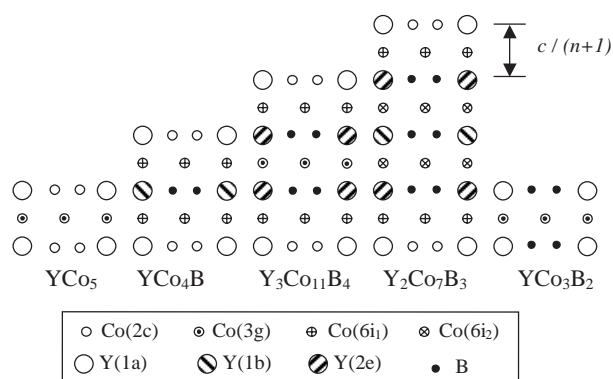
**Figure 1.** Projection of the crystallographic structures showing the different cobalt sites of the $Y_{n+1}Co_{3n+5}B_{2n}$ ($n = 0, 1, 2, 3$ and $\infty$) compounds. The figure is a projection of the structures along the [1 1 0] axis.

sites in $RCo_4B$ and the 1a and 2e sites in $R_3Co_{11}B_4$. The crystal structure of $R_2Co_7B_3$ is even more complex, with three inequivalent R sites located in Wyckoff positions 1a, 1b, and 2e. A detailed representation of the $R_3Co_{11}B_4$ and $R_2Co_7B_3$ structures is given in figure 2. In these structures, the cobalt atoms occupy four different crystallographic positions, the 2c, $6i_1$, 3g and $6i_2$. In fact, three kinds of cobalt atomic site are found in $R_{n+1}Co_{3n+5}B_{2n}$, the Co(2c), Co($6i_1$) and Co(3g or $6i_2$) sites have zero, one, and two neighbouring B layers, respectively. In Y–Co compounds, the magnetic behaviour of cobalt is strongly correlated to the composition of its neighbourhood [3, 4]. It is has been shown that, in the ternary system, when B is included, the presence of boron induces a hybridization of the B(2p) and Co(3d) orbitals [5]. In addition, the substitution of boron for cobalt influences the magnetic
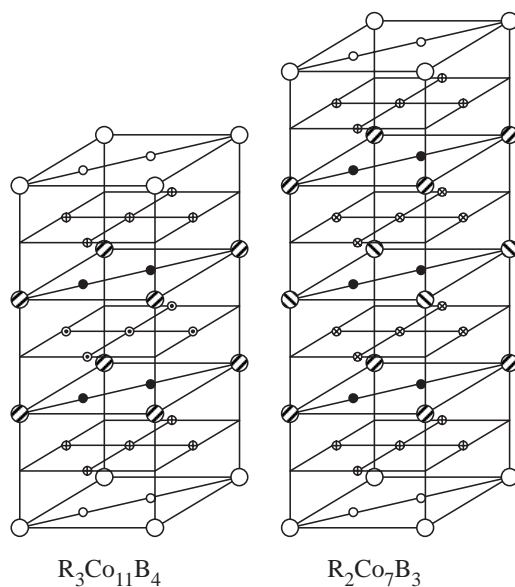


**Figure 2.** Crystal structure of the $R_3Co_{11}B_4$ and $R_2Co_7B_3$ phases. For the nature of the crystal sites, see legend in figure 1.

behaviour of the cobalt atoms by modifying the interatomic distance and the nature of the nearest neighbours.

Previous experimental studies have indicated that the contribution of the different cobalt site to the magnetic behaviour is seriously dependent on the nature of the crystal site. For example, the anisotropy constant $K_1$ was found to depend upon the nature of the crystal site in the $R_{n+1}Co_{3n+5}B_{2n}$ compounds [6–9]. Band structure calculations have also shown major differences in the role played by each cobalt site on the electronic structure [10, 11] in the $Y_{n+1}Co_{3n+5}B_{2n}$ compounds. A large variety in the cobalt magnetic moment, depending on the crystal site, is predicted, as well as the disappearance of the magnetism for the cobalt atom in the $YCo_3B_2$ compound. The evolution of the other magnetic characteristics, such as the exchange interactions [12], the magnetization [13] or the susceptibility [14], has also shown large changes upon substitution of boron for cobalt.

We report on magnetic measurements and high-resolution neutron diffraction on the $Y_{n+1}Co_{3n+5}B_{2n}$ compounds. To our knowledge, this is the first investigation of this family of compounds by means of powder neutron diffraction. For all the compounds studied, the crystal structure is determined using neutron diffraction experiments performed above the Curie temperature and the magnetic structure is obtained at 2 K.

## 2. Experimental details

The polycrystalline phases of the $Y_{n+1}Co_{3n+5}B_{2n}$ compounds ($n = 1, 2, 3$ and $\infty$) were prepared by melting the starting materials of 99.9% or better purity in an arc furnace. The ingots were remelted in a high-frequency furnace under an argon atmosphere for better homogeneity. Small pieces of the ingots were wrapped in Ta foil, sealed in an evacuated silica tube, and annealed for one month at 1273 °C. The phase purity of the samples was checked by x-ray diffraction using a Guinier focusing camera and the $K\alpha_1$ radiation of iron ($\lambda = 1.9373$ Å).

The neutron experiments were performed at the Institut Laue Langevin in Grenoble, France, on the *D2B* and *D1A* instruments, a description of which can be found elsewhere [15]. Both spectrometers are very high-resolution powder diffractometers operating with a take-off angle of the monochromator of 122° and 135° for *D1A* and *D2B*, respectively. In the configuration used, the resolution of both spectrometers is about 0.3° (FWHM) at 90°. The measurements were carried out at a wavelength of $\lambda = 1.91$ and 1.59 Å for *D1A* and *D2B*, respectively. The neutron detection is performed with $^3$He counting tubes spaced at 6° and 2.5° intervals for *D1A* and *D2B*, respectively. The complete diffraction pattern is obtained by scanning over the whole $2\theta$ range. The data were analysed with the Rietveld structure refinement program FULLPROF [16].

In order to reduce absorption by the samples, several steps were taken into account:

- during the synthesis, we have chosen to use $^{11}$B instead of $^{10}$B in order to lower the neutron absorption cross section.
- the effects of cobalt absorption were minimized; firstly by using a small sample container of only 5 mm in diameter leading to lower the absorption, secondly the density of the sample in the sample holder was only 50% of the bulk density.

Finally the Co atomic concentration is only about 50% in these compounds.

Naturally, the problem of the absorption has been taken into account according to [17] and [18]. The transmission factor $A_{hkl}$ has been calculated according to the formula proposed by Hewat [18] and this leads to adjustments of the Debye–Waller factor $B_{DB}$ at the end of the refinement. The correction to the Debye–Waller factor is calculated to be $\Delta B_{DB} = 0.25$ Å$^2$

for $Y_3Co_{11}B_4$, which is the most absorbing compound studied here, and $\Delta B_{DB} = 0.20$ Å$^2$ for $YCo_3B_2$.

The typical Debye–Waller thermal factors $B_{DB}$, obtained at 4 K after correction for the absorption, are 0.3, 0.45 and 0.8 Å$^2$ for Y, Co and B respectively. The high-temperature values are 0.8, 1 and 1.6 Å$^2$ for Y, Co and B respectively.

The Curie temperature ($T_C$) was measured using a Faraday balance with a heating and cooling rate of 5 K min$^{-1}$. Magnetization measurements were performed using the extraction method in a continuous field up to 7 T. The saturation magnetization ($M_s$) was determined by extrapolation at zero field of the isothermal curve.

## 3. Results and discussion

Inspection of the x-ray diffraction patterns reveals that, after annealing, $YCo_4B$ ($n = 1$), $Y_3Co_{11}B_4$ ($n = 2$) and $YCo_3B_2$ ($n = \infty$) are single phase and can be indexed in the related $Ce_{n+1}Co_{3n+5}B_{2n}$-type structures [2]. The presence of a small quantity of $Y_3Co_{11}B_4$ was detected in the $Y_2Co_7B_3$ sample. The room temperature lattice parameters of the $Y_{n+1}Co_{3n+5}B_{2n}$ compounds are given in table 1. The lattice parameter $a$ is found to be virtually constant in the boron containing samples. This indicates that the Y–B distances in the $Y_{n+1}Co_{3n+5}B_{2n}$ compounds are unchanged as the amount of boron increases. The $c/(n + 1)$ parameter represents the distance between two R-containing planes along the $c$ axis (figure 1). Table 1 shows that the $c/(n + 1)$ parameter decreases upon the substitution of boron for cobalt. This behaviour reveals a decrease in the distance between R-containing planes along the $c$ axis as the boron concentration increases. As a consequence, we observe a volume reduction of the site of the cobalt 3g, 6i$_1$, and 6i$_2$ sites and a decrease of the interatomic distances between these atoms and the B and Y atoms. The density of the $Y_{n+1}Co_{3n+5}B_{2n}$ phases is found to decrease upon the substitution of boron for cobalt. To understand the changes in the interatomic distances between cobalt and boron atoms with increasing boron concentration, the crystal structures of the $Y_{n+1}Co_{3n+5}B_{2n}$ compounds ($n \geqslant 2$) have been determined by neutron diffraction measurements above the magnetic ordering temperature. Table 2 gives the crystallographic positions, as well as the reliability factors, obtained from our Rietveld refinement of the neutron diffraction data. A full description of the Rietveld method used in this article can be found elsewhere [19]. The agreement factors used in this article are defined as $R_{exp} = [(N - P + C)/\Sigma_i \omega_i y_i^2]^{1/2}$, $R_{wp} = [\Sigma_i \omega_i |y_I - y_{ci}|^2/\Sigma_i \omega_i |y_i|^2]^{1/2}$ and $R_p = \Sigma_i |y_I - y_{ci}|/\Sigma_i |y_i|$ where $y_i$ and $y_{ci}$ are the observed and calculated counts at the $i$th step of the pattern respectively. $N - P + C$ is the number of degrees of freedom ($N$ is the number of points in the pattern, $P$ the number of refined parameters and $C$ the number of constraint functions). The weights for the observations are calculated as $\omega_i = 1/y_i$. The Bragg agreement factor is defined as $R_B = \Sigma_k |I_k - I_{ck}|/\Sigma_k |I_k|$ where $I_k$ and $I_{ck}$ are the observed and calculated integrated intensity at the $k$th reflection, respectively. The magnetic reliability

**Table 1.** Lattice parameters and density of the $Y_{n+1}Co_{3n+5}B_{2n}$ compounds determined from x-ray diffraction at room temperature.

|                          | $YCo_5$ $n = 0$ | $YCo_4B$ $n = 1$ | $Y_3Co_{11}B_4$ $n = 2$ | $Y_2Co_7B_3$ $n = 3$ | $YCo_3B_2$ $n = \infty$ |
|--------------------------|-----------------|------------------|-------------------------|----------------------|-------------------------|
| $a$ (Å)                  | 4.937 (1)       | 5.026 (1)        | 5.041 (2)               | 5.036 (2)            | 5.031 (1)               |
| $c$ (Å)                  | 3.978 (1)       | 6.899 (1)        | 9.853 (4)               | 12.899 (5)           | 3.034 (1)               |
| $c/(n + 1)$ (Å)          | 3.978           | 3.450            | 3.284                   | 3.225                | —                       |
| Density (g cm$^{-3}$)    | 7.58            | 7.38             | 7.34                    | 7.30                 | 7.17                    |

**Table 2.** Crystal structure and reliability factors obtained by Rietveld refinement of the neutron diffraction pattern measured above the Curie temperature.

|  | $YCo_4B^a$ 300 K D1A | $Y_3Co_{11}B_4$ 383 K D2B | $Y_2Co_7B_3$ 373 K D2B |
|---|---|---|---|
| Crystal structure |  |  |  |
| $z_{Co}$ (6i$_1$) | 0.283 (2) | 0.199 (3) | 0.152 (3) |
| $z_{Co}$ (6i$_2$) | — | — | 0.392 (3) |
| $z_B$ (4h) | — | 0.351 (1) | 0.266 (2) |
| Reliability factors (%) |  |  |  |
| $R_p$ (%) | 2.1 | 4.6 | 4.8 |
| $R_{wp}$ (%) | 4.7 | 8.4 | 8.6 |
| $R_{exp}$ (%) | 4.0 | 6.0 | 6.2 |
| $R_{Bragg}$ (%) | 6.8 | 9.5 | 12.2 |

[a]From [29].

factor $R_{mag}$ is defined as $R_{mag} = \Sigma_k |I_k - I_{ck}| / \Sigma_k |I_k|$ where $I_k$ and $I_{ck}$ are the observed and calculated magnetic contributions to the integrated intensity at the $k$th reflection respectively. The neutron diffraction pattern of $Y_2Co_7B_3$ confirms the presence of the $Y_3Co_{11}B_4$ phase as an impurity. The Rietveld refinement of the $Y_2Co_7B_3$ pattern indicates that the atomic percentage of the impurity is about 10%. The interatomic distances are determined from the crystal structure. The Co–B near-neighbour interatomic distances observed in $Y_{n+1}Co_{3n+5}B_{2n}$ are particularly short, i.e., less than 2.1 Å and indicate a strong bond between the cobalt and boron atoms. We have studied the evolution of the Co(6i$_{1,2}$)–B distance as a function of the boron concentration. This interatomic distance is the shortest distance between cobalt and boron in the $Y_{n+1}Co_{3n+5}B_{2n}$ compounds. The Co(6i$_{1,2}$)–B distance is found to be almost constant in the $YCo_4B$, $Y_3Co_{11}B_4$ and $YCo_3B_2$ compounds at about 2.08 Å. In contrast, it is significantly reduced to 2.01 Å between the Co(6i$_2$) and B(2d) in the $Y_2Co_7B_3$ compounds. Such a value represents a very short interatomic distance in comparison with other existing compounds in the Co–B binary or Y–Co–B ternary systems. For example, the shortest Co–B distance observed in compounds of the Y–Co–B phase diagram [20] is about 2.04 Å. The existence of such a short Co–B distance in the $Y_2Co_7B_3$ structure indicates a break in the regular stacking of the boron-containing planes along the $c$ axis in comparison with the compounds of $Y_{n+1}Co_{3n+5}B_{2n}$ for $n < 3$. The occurrence of a short interatomic distance between the Co(6i$_2$) and B(2d) atoms may also indicate some defaults in the stacking of the boron-containing planes and may partly explain the formation of the $Y_3Co_{11}B_4$ phase as an impurity in the $Y_2Co_7B_3$ compound. It should be noted that, to date, in the $Y_{n+1}Co_{3n+5}B_{2n}$ series of compounds, no structure with $3 < n < \infty$ has been stabilized. We have demonstrated that the Co–B distances in the $Y_{n+1}Co_{3n+5}B_{2n}$ phases decrease as $n$ increases. The reason for the non-stability of the $Y_{n+1}Co_{3n+5}B_{2n}$ phases with $3 < n < \infty$ may be that the existence of such a short Co–B distance constitutes a critical parameter in the stabilization of other structure with $3 < n < \infty$. The Co–Y distances cannot be the critical parameter because the comparison of the Co–Y distances, calculated for the $Y_2Co_7B_3$ structure, indicates that the shortest distance of 2.85 Å is of the same magnitude as those observed in other ternary Y–Co–B compounds such as $YCo_4B_4$, $YCo_2B_2$ [20, 21] and $Y_2Co_{14}B$ [22, 23]. Hence, the Co–Y distance cannot be regarded as critical in the $Y_{n+1}Co_{3n+5}B_{2n}$ phases. Finally, the B–Y distances are found to be comparable to those observed in $YCo_4B_4$ and even larger than the 2.76 Å value observed in $YCo_2B_2$. We conclude that only the Co–B distances are observed to be unusually short as compared to other compounds in the Y–Co–B ternary phase diagram.
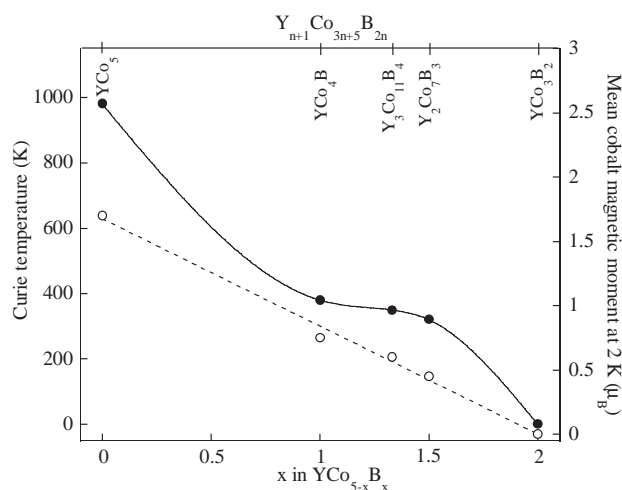
**Figure 3.** Dependence of the Curie temperature and of the mean magnetic moment per cobalt atoms at 2 K on the boron concentration. The full circles refer to the left axis and correspond to the Curie temperature. The open circles represent the mean Co magnetic moment corresponding to the right axis. The results are plotted for the $Y_{n+1}Co_{3n+5}B_{2n}$ ($YCo_{5-x}B_x$) compounds for $n = 0, 1, 2, 3$ and $\infty$ ($x = 0, 1, 1.33, 1.5$ and 2).
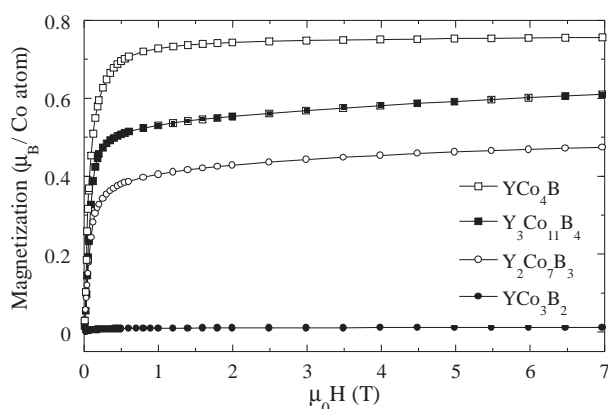


**Figure 4.** Magnetization curves measured at 2 K in the $Y_{n+1}Co_{3n+5}B_{2n}$ compounds for $n = 1, 2, 3$ and $\infty$.

The magnetic properties of cobalt in the $Y_{n+1}Co_{3n+5}B_{2n}$ compounds are strongly modified when the boron concentration increases. Figure 3 gives the evolution with boron content of $T_C$ and the mean magnetic moment per cobalt atom at 2 K deduced from the saturation magnetization (figure 4). The substitution of boron for cobalt induces a dramatic decrease in magnetization of the $Y_{n+1}Co_{3n+5}B_{2n}$ compounds. Specifically, the magnetization curve obtained for $YCo_3B_2$ at 2 K confirms that it is paramagnetic above this temperature. We have investigated the magnetic behaviour of $YCo_3B_2$ by neutron diffraction at 2 K. Figure 5 presents the results of the Rietveld analysis of the neutron diffraction pattern, an analysis in which only the crystal structure has been used. The addition of an ordered magnetic structure
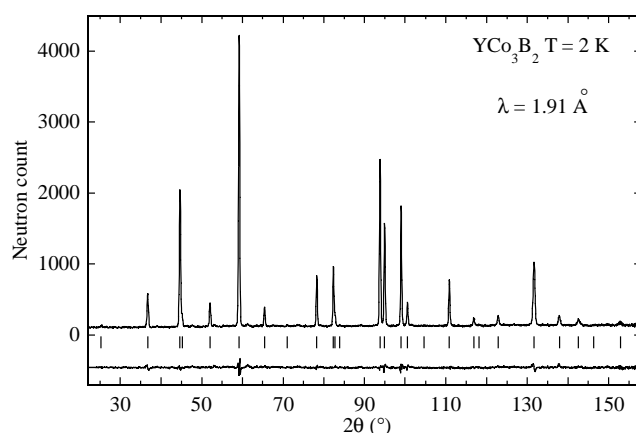
**Figure 5.** Neutron powder diffraction pattern of $YCo_3B_2$ recorded at 2 K on the *D1A* spectrometer. The drawn pattern refers to the experimental data. The difference between the experimental data and the calculated pattern is plotted on the lower part of the figure. The row of streaks refers to the nuclear contribution to the diffraction pattern. The reliability factors of this Rietveld refinement are equal to 4.5, 5.8, 6.9 and 2.5 (%) for $R_p$, $R_{exp}$, $R_{wp}$, and $R_{Bragg}$ respectively.

for this compound does not improve the quality of the fit or the reliability factors. This analysis shows that the $YCo_3B_2$ is paramagnetic down to 2 K and confirms the results obtained on this compound by nuclear magnetic resonance [24], magnetic susceptibility [25] and specific heat [26] measurements. Our results also demonstrate that the non-zero saturation magnetization reported for $YCo_3B_2$ at 2 K in [25] is due to the contribution of an impurity phase in their sample. Our neutron diffraction measurements are also in good agreement with the magnetic behaviour predicted by electronic structure calculations on $YCo_3B_2$ [10]. The magnetic behaviour of $YCo_3B_2$ indicates that the Co(3g) atoms do not carry any significant magnetic moment. As shown in figure 1, in the $YCo_3B_2$ structure, the Co(3g) atoms are surrounded in the $c$ axis direction, by two boron-containing planes. Hence, we conclude that an important charge transfer occurs between the B and Co(3g) atoms via B(2p)–Co(3d) hybridization. Our results are in good agreement with previous neutron diffraction measurement performed on $TbCo_3B_2$ [27, 28]. In this compound, Caspi *et al* [27] have proposed a very small magnetic moment of about 0.1 $\mu_B$ for the Co(3g) atoms, a moment which is of the order of the error bar and could be related to the existence of a cobalt magnetic moment induced by the magnetic rare earth. Our results may also to be compared with the magnetic structure reported in $YCo_4B$ [29], in which a magnetic moment of 0.6 $\mu_B$ has been found for the cobalt atoms located in the $6i_1$ position [29]. In this structure, the $6i_1$ sites have one plane containing boron atoms in their environment (figure 1). The cobalt atoms situated on the 2c crystallographic site, which has no boron as first neighbour, carry a much larger magnetic moment of 1.6 $\mu_B$. Consequently, a link between the magnetic moment of the cobalt atoms and the number of boron atoms in the cobalt environment is expected. $Y_3Co_{11}B_4$ and $Y_2Co_7B_3$ are excellent candidates to verify this hypothesis because they have cobalt atoms with 0, 1 or 2 boron-containing planes as their nearest neighbours. Thus, a large variety of magnetic moments for the cobalt atoms, depending on the nature of the crystal site, is expected in both $Y_3Co_{11}B_4$ and $Y_2Co_7B_3$. We have performed neutron diffraction measurements at 2 K on the $Y_3Co_{11}B_4$ and $Y_2Co_7B_3$ compounds. The fit of the powder diffraction pattern recorded above the Curie temperature has shown that no disorder between the Co and B atoms exists. The atomic positions are either fully occupied by Co or fully occupied by B atoms. Consequently the occupancy of the

**Table 3.** Magnetic features obtained by Rietveld refinement of the neutron diffraction pattern measured at 2 K in the *D2B* diffractometer for the $Y_3Co_{11}B_4$ and $Y_2Co_7B_3$ samples. The standard deviations on the cobalt magnetic moment are estimated as $\pm 0.15\ \mu_B$[a]. Earlier reported results on $YCo_4B$ and $YCo_5$ are given for comparison.

| | $YCo_5$[b] $n=0$ | $YCo_4B$[c] $n=1$ | $Y_3Co_{11}B_4$ $n=2$ | $Y_2Co_7B_3$ $n=3$ | $YCo_3B_2$ $n=\infty$ |
|---|---|---|---|---|---|
| $a$ (Å) | 4.928 (1) | 5.012 (2) | 5.038 (2) | 5.035 (1) | 5.018 (1) |
| $c$ (Å) | 3.971 (1) | 6.871 (2) | 9.836 (4) | 12.860 (5) | 3.022 (1) |
| Cobalt magnetic moments ($\mu_B$) | | | | | |
| Co(2c) | 1.8 (1) [d] | 1.6 (2) | 1.7 (2) | 1.5 (2) | — |
| Co(3g) | 1.7 (1) [d] | — | 0.1 (2) | — | 0 |
| Co($6i_1$) | — | 0.6 (2) | 0.7 (2) | 0.5 (2) | — |
| Co($6i_2$) | — | — | — | 0 | — |
| Reliability factors (%) | | | | | |
| $R_p$ | | 2.5 | 5.1 | 4.6 | 4.5 |
| $R_{exp}$ | | 4.7 | 6.7 | 6.0 | 5.8 |
| $R_{wp}$ | | 3.3 | 8.7 | 8.4 | 6.9 |
| $R_{Bragg}$ | | 8.4 | 9.6 | 8.1 | 2.5 |
| $R_{mag}$ | | 15.5 | 13.9 | 16.8 | — |

[a] For more details on the standard deviation of the Rietveld refinement, see [42] and [43].
[b] From [44].
[c] From [45].
[d] Polarized neutron.

sites was not refined at low temperature. This has enabled us to reduce the number of refined parameters and gives confidence in the Rietveld refinement results obtained at low temperature. Nothing else has been deduced or constrained from these high-temperature measurements. The (*x*, *y*, *z*) atomic coordinates, as well as the lattice parameters, have also been refined at low temperature. During the refinements, the crystallographic structure was based on the results obtained above the Curie temperature. The only atomic parameters refined were the (*x*, *y*, *z*) ones given in table 2 and the magnetic moments. All the magnetic moments were not refined at the same time, in particular the magnetic moment on the Co(3g) site in $Y_3Co_{11}B_4$ was only let free at the end of the refinement, but this moment was not found to deviate significantly from zero as shown in table 3. Examples of patterns recorded on the *D2B* diffractometer are given in figures 6 and 7 and the results of the Rietveld refinements are listed in table 3. It should be noted that the analysis of $Y_3Co_{11}B_4$ was performed first and the results were used to take into account the presence of this phase as an impurity in the $Y_2Co_7B_3$ sample. Good agreement is found between the magnetic moments obtained by Rietveld refinement and the saturation magnetization presented in figures 3 and 4. Table 3 reveals a relatively high value of the $R_{mag}$ factor in the Rietveld refinement. This results because the structure exhibits, even at 2 K, only a small magnetic contribution to the neutron diffraction scattering in comparison to the nuclear scattering. A variety of magnetic moments is found for the cobalt atoms in the $Y_3Co_{11}B_4$ and $Y_2Co_7B_3$ compounds. The Co(2c) atoms are not significantly affected by the substitution of boron for cobalt. The Co atoms exhibit a magnetic moment which is rather close to those measured, for the same crystal site, in $YCo_5$ [30] or $YCo_4B$ [29]. This confirms that the Co(2c)–B distances are large enough to prevent any direct effect of boron on the magnetism of the cobalt atoms found on the 2c position in all the superstructure of the $Y_{n+1}Co_{3n+5}B_{2n}$ compounds. We can also expect that the exchange interactions between the cobalt atoms located on 2c sites are not significantly affected by the substitution of boron for cobalt. Table 3 shows that the magnetic
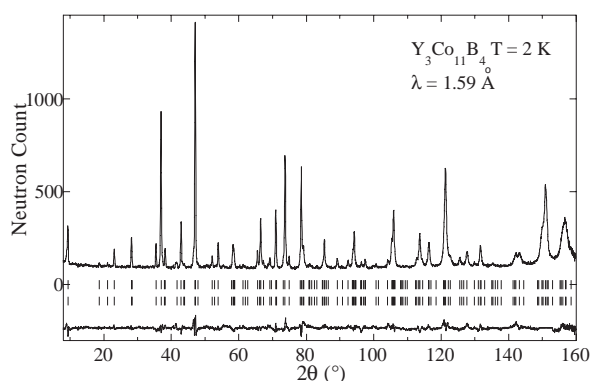
**Figure 6.** High resolution neutron powder diffraction pattern of $Y_3Co_{11}B_4$ recorded at 2 K (*D2B*). The drawn pattern refers to the experimental data. The difference between the experimental data and the calculated pattern is plotted on the lower part of the figure. The two rows of streaks refer to the nuclear and magnetic contribution of $Y_3Co_{11}B_4$ to the diffraction pattern.

moments of the cobalt atoms located on the 3g, $6i_1$ and $6i_2$ sites are affected by the presence of boron atoms in their neighbouring planes. They all exhibit smaller magnetic moments than the cobalt atoms located on the 2c site. Two different magnetic behaviours of these cobalt atoms are observed: firstly, the cobalt atoms on the $6i_1$ site have a magnetic moment of about 0.6 $\mu_B$; secondly, no significant magnetic moment is observed for the Co(3g) and Co($6i_2$) sites. These results confirm the link between the number of boron near neighbours and the magnetic moment of the cobalt atoms. In particular, the study of $Y_3Co_{11}B_4$ and $Y_2Co_7B_3$ confirms the results found for $YCo_3B_2$, i.e. that if the cobalt atoms are surrounded by two boron containing planes they are non-magnetic. The presence of cobalt atoms on the 2c site in $Y_3Co_{11}B_4$ and $Y_2Co_7B_3$ may be the main origin of the magnetic order in these compounds, compared with the paramagnetic state of $YCo_3B_2$. It is to be noticed that our results on cobalt magnetic moments are in good agreement with theoretical calculations [11, 31, 32]. As an example, the experimental Co magnetic moments determined for $Y_3Co_{11}B_4$ are in excellent agreement with the band structure calculation of Kowalczyk and co-workers [31, 32] on isotype compounds $Nd_3Co_{11}B_4$ or $Tm_3Co_{11}B_4$. The magnitude of the Co magnetic moments are also in excellent agreement with earlier reported experimental results of $^{59}$Co nuclear magnetic resonance [33, 34, 35].

Our neutron diffraction study also enables us to determine the easy magnetization direction in the $Y_{n+1}Co_{3n+5}B_{2n}$ compounds. At 2 K, the orientation of the cobalt magnetization is along the c axis in both $Y_3Co_{11}B_4$ and $Y_2Co_7B_3$. These results are in good agreement with the easy direction of magnetization obtained by Ogata *et al* from high-magnetic-field magnetic measurements [7] or by Maruyama *et al* by NMR studies [36]. The same behaviour has been observed at 2 K for the other members of the $Y_{n+1}Co_{3n+5}B_{2n}$ compounds. In the case of $YCo_5$, previous studies have demonstrated that the easy magnetization direction is determined mainly by the contribution of the Co(2c) site to the magnetocrystalline anisotropy [37, 38]. The same behaviour has been detected at high temperature in $YCo_4B$ [39, 40]. Because our results demonstrate that the magnetic moments of the cobalt atoms located on 2c sites are not significantly affected by the substitution of boron for cobalt, it appears that the easy magnetization direction in the $Y_3Co_{11}B_4$ and $Y_2Co_7B_3$ is also determined by the contribution of the Co(2c) atoms. It should also be noted that, in $YCo_4B$, a spin reorientation occurs when the temperature decreases [29, 41]. It has been established that the change in the easy magnetization direction is a consequence of competition between the contribution of the cobalt atoms on the 2c and 6i
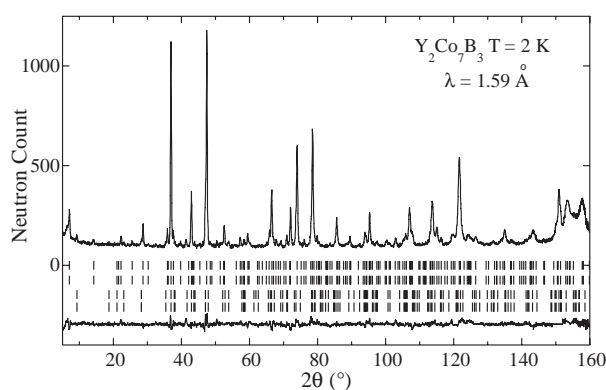
**Figure 7.** High-resolution neutron powder diffraction pattern of $Y_2Co_7B_3$ recorded at 2 K (*D2B*). The drawn pattern refers to the experimental data. The difference between the experimental data and the calculated pattern is plotted on the lower part of the figure. The first two rows of streaks refer to the nuclear and magnetic contribution of $Y_2Co_7B_3$ to the diffraction pattern and the two last ones represent the nuclear and magnetic contribution of the $Y_3Co_{11}B_4$ (impurity) respectively.

sites to the magnetocrystalline anisotropy [40]. In $Y_3Co_{11}B_4$ and $Y_2Co_7B_3$, no spin reorientation is observed at any temperature. This behaviour can indicate that, at any temperature, the contribution of the 2c site imposes the easy magnetization direction in $Y_3Co_{11}B_4$ and $Y_2Co_7B_3$.

Our neutron diffraction measurements disagree with some results reported for $Tb_3Co_{11}B_4$ and $Tb_2Co_7B_3$ [28]. In particular, a rather low magnetic moment was reported on the Co(2c) atoms and a rather high magnetic moment on the Co($6i_1$) of $Tb_2Co_7B_3$ [28]. This behaviour can be explained, as suggested by the authors, by the low resolution in their neutron diffractometer and by their failure to include impurities in their refinements. The high-resolution diffractometer used in this work and the inclusion of $Y_3Co_{11}B_4$ as an impurity phase in the refinement of the $Y_2Co_7B_3$ diffraction pattern permit us to be confident of our results. The close agreement of the magnetization obtained from the neutron diffraction results and those deduced from magnetization measurements is another argument in favour of our present results. Finally, the consistency between the results obtained for all the $Y_{n+1}Co_{3n+5}B_{2n}$ phases is further proof of the reliability of our analysis.

## 4. Conclusion

According to the neutron diffraction investigation, the $Y_{n+1}Co_{3n+5}B_{2n}$ compounds can be considered as ordered stoichiometric compounds. $YCo_5$ ($n = 0$), $YCo_4B$ ($n = 1$), $Y_3Co_{11}B_4$ ($n = 2$) and $YCo_3B_2$ ($n = \infty$) have been analysed but no phases with $3 < n < \infty$ have been observed. The reason for the non-stability of such phases may be the extremely short 2.01 Å Co–B distances found in $Y_2Co_7B_3$. The magnetization measurements indicated that the magnetization of the $Y_{n+1}Co_{3n+5}B_{2n}$ compounds is significantly reduced as $n$ increases. The $YCo_3B_2$ phase is even found to be paramagnetic at 2 K. The reduction of the $Y_{n+1}Co_{3n+5}B_{2n}$ magnetization upon the substitution of boron for cobalt is not only due to the replacement of a magnetic cobalt atom by non-magnetic boron, but also because the magnetic moment of the remaining cobalt atoms is also significantly reduced by the hybridization of the Co(3d) electronic orbitals with the 2p orbitals of the surrounding boron atoms. The cobalt magnetic moments decreases as the number of boron neighbours increases. When the cobalt atoms are surrounded by two boron-containing planes, the magnetic moments of the cobalt atoms are paramagnetic. This is the case for $YCo_3B_2$ and for some of the cobalt atoms in $Y_3Co_{11}B_4$ and $Y_2Co_7B_3$.

## Acknowledgments

## References

[1] Buschow K H J 1997 *Handbook of Magnetic Materials* vol 10 ed K H J Buschow (Amsterdam: Elsevier) p 463
[2] Kuz'ma Yu B and Bilonizhko N S 1974 *Sov. Phys–Crystallogr.* **18** 447
[3] Strnat K J 1988 *Ferromagnetic Materials* vol 4 ed E P Wohlfart and K H J Buschow (Amsterdam: Elsevier) p 131
[4] Kakol Z, Figiel Z and Turek K 1984 *IEEE Trans. Magn.* **20** 1605
[5] Duc N H and Givord D 1995 *J. Magn. Magn. Mater.* **151** L13
[6] Smit H H A, Thiel R C and Buschow K H J 1988 *J. Phys. F: Met. Phys.* **18** 295
[7] Ogata H, Ido H and Yamauchi H 1993 *J. Appl. Phys.* **73** 5911
[8] Kowalczyk A 1994 *Phys. Status Solidi* b **181** K73
[9] Oda K, Sugiyama K, Kindo K, Hong N M, Asano H, Nashima O and Ido H 1995 *J. Magn. Magn. Mater.* **140–144** 947
[10] Yamada H, Terao K, Nakazawa H, Kitagawa I, Suzuki N and Ido H 1998 *J. Magn. Magn. Mater.* **183** 94
[11] Szajek A 1998 *J. Magn. Magn. Mater.* **185** 322
[12] Maruyama F 1999 *Jpn. J. Appl. Phys.* **38** 1380
[13] Kowalczyk A 1993 *Phys. Status Solidi* b **180** K19
[14] Burzo E, Pop V, Borodi C C and Ballou R 1994 *IEEE Trans. Magn.* **30** 628
[15] Hewat A 1986 *Mater. Sci. Forum* **9** 69
[16] Rodriguez-Carjaval J 1993 *Physica* B **192** 55
[17] Rousse K D and Cooper M J 1970 *Acta Crystallogr.* A **26** 682
[18] Hewat A 1979 *Acta Crystallogr.* A **35** 248
[19] McCusker L B, Von Dreele R B, Cox D E, Louër D and Scardi P 1999 *J. Appl. Crystallogr.* **32** 36
[20] Rogl P 1984 *Handbook of the Physics and the Chemistry of Rare Earths* vol 6 ed K A Gschneidner Jr and L Eyring (Amsterdam: North-Holland) p 335
[21] Villars P and Calvert L D 1985 *Pearson's Handbook of Crystallographic Data for Intermetallic Phases* vol 2 (Materials Park: ASM)
[22] Le Roux D, Vincent H, L'Héritier P and Fruchart R 1985 *J. Physique* **46** 243
[23] Hong N M, Franse J J M and Thuy N P 1989 *J. Less-Common Met.* **155** 151
[24] Ichinose K, Watanabe N, Shimizu K and Ido H 1998 *J. Magn. Magn. Mater.* **177–181** 1113
[25] Ido H, Yamauchi H, Cheng S F, Sankar S G and Wallace W E 1991 *J. Appl. Phys.* **70** 6540
[26] Perthold W, Hong N M, Michor H, Hilscher G, Ido H and Asano H 1996 *J. Magn. Magn. Mater.* **157–158** 649
[27] Caspi E, Pinto H, Kuznietz M, Ettedgui H, Melamud M, Felner I and Shaked H 1998 *J. Appl. Phys.* **83** 6733
[28] Caspi E, Pinto H and Melamud M 2000 *J. Appl. Phys.* **87** 416
[29] Chacon C and Isnard O 2001 *J. Appl. Phys.* **89** 71
[30] Franse J J M and Radwanski R J 1993 *Handbook of Magnetic Materials* vol 7 ed K H J Buschow (Amsterdam: Elsevier) p 307
[31] Kowalczyk A and Jezierski A 1998 *J. Magn. Magn. Mater.* **182** 137
[32] Szajek A, Kowalczyk A and Smardz L 2001 *J. Magn. Magn. Mater.* **223** 119
[33] Maruyama F, Nagai H, Amako Y, Yoshie H and Adachi K 1998 *Japan. J. Appl. Phys.* **37** 1825
[34] Kapusta Cz, Rosenberg M and Buschow K H J 1992 *J. Alloys Compounds* **187** 409
[35] Ido H 1995 *Kotai Butsuri* **30** 875 (in Japanese)
[36] Maruyama F, Nagai H, Amako Y, Yoshie H and Adachi K 1998 *Japan. J. Appl. Phys.* **37** 2492
[37] Déportes J, Givord D, Schweizer J and Tasset F 1976 *IEEE Trans. Magn.* **12** 1000
[38] Alameda J, Givord D, Lemaire R and Lu Q 1981 *J. Appl. Phys.* **52** 2079
[39] Thang C V 1996 *PhD Thesis* University of Amsterdam
[40] Cadogan J M, Li H S, Campbell S J and Jing J 1992 *Solid State Commun.* **81** 121
[41] Chacon C and Isnard O 2000 *J. Solid State Chem.* **154** 242
[42] Bérar J F and Lelann P 1991 *J. Appl. Crystallogr.* **24** 1
[43] Bérar J F 1992 *Proc. Int. Conf. on Accuracy in Powder Diffraction II* (NIST Gaithersburg, MD, May 26–29) p 63
[44] Tasset F 1975 *PhD Thesis* University of Grenoble
[45] Chacon C 2000 *PhD Thesis* University of Grenoble